



OPEN

Investigation on performance of particle swarm optimization (PSO) algorithm based fuzzy inference system (PSOFIS) in a combination of CFD modeling for prediction of fluid flow

Meisam Babanezhad^{1,2,3}, Iman Behroyan^{4,5}, Ali Taghvaie Nakhjiri⁶, Azam Marjani^{7,8}✉, Mashallah Rezakazemi⁹, Amir Heydarinasab⁶ & Saeed Shirazian¹⁰

Herein, a reactor of bubble column type with non-equilibrium thermal condition between air and water is mechanistically modeled and simulated by the CFD technique. Moreover, the combination of the adaptive network (AN) trainer with the fuzzy inference system (FIS) as the artificial intelligence method calling ANFIS has already shown potential in the optimization of CFD approach. Although the artificial intelligence method of particle swarm optimization (PSO) algorithm based fuzzy inference system (PSOFIS) has a good background for optimizing the other fields of research, there are not any investigations on the cooperation of this method with the CFD. The PSOFIS can reduce all the difficulties and simplify the investigation by elimination of the additional CFD simulations. In fact, after achieving the best intelligence, all the predictions can be done by the PSOFIS instead of the massive computational efforts needed for CFD modeling. The first aim of this study is to develop the PSOFIS for use in the CFD approach application. The second one is to make a comparison between the PSOFIS and ANFIS for the accurate prediction of the CFD results. In the present study, the CFD data are learned by the PSOFIS for prediction of the water velocity inside the bubble column. The values of input numbers, swarm sizes, and inertia weights are investigated for the best intelligence. Once the best intelligence is achieved, there is no need to mesh refinement in the CFD domain. The mesh density can be increased, and the newer predictions can be done in an easier way by the PSOFIS with much less computational efforts. For a strong verification, the results of the PSOFIS in the prediction of the liquid velocity are compared with those of the ANFIS. It was shown that for the same fuzzy set parameters, the PSOFIS predictions are closer to the CFD in comparison with the ANFIS. The regression number (R) of the PSOFIS (0.98) was a little more than that of the ANFIS (0.97). The PSOFIS showed a powerful potential in mesh density increment from 9477 to 774,468 and accurate predictions for the new nodes independent of the CFD modeling.

¹Institute of Research and Development, Duy Tan University, Da Nang 550000, Vietnam. ²Faculty of Electrical – Electronic Engineering, Duy Tan University, Da Nang 550000, Vietnam. ³Department of Artificial Intelligence, Shunderman Industrial Strategy Co., Tehran, Iran. ⁴Faculty of Mechanical and Energy Engineering, Shahid Beheshti University, Tehran, Iran. ⁵Department of Computational Fluid Dynamics, Shunderman Industrial Strategy Co., Tehran, Iran. ⁶Department of Petroleum and Chemical Engineering, Science and Research Branch, Islamic Azad University, Tehran, Iran. ⁷Department for Management of Science and Technology Development, Ton Duc Thang University, Ho Chi Minh City, Vietnam. ⁸Faculty of Applied Sciences, Ton Duc Thang University, Ho Chi Minh City, Vietnam. ⁹Faculty of Chemical and Materials Engineering, Shahrood University of Technology, Shahrood, Iran. ¹⁰Laboratory of Computational Modeling of Drugs, South Ural State University, 76 Lenin prospect, Chelyabinsk, Russia 454080. ✉email: azam.marjani@tdtu.edu.vn

Various sorts of reactors have been designed and exploited for multi-phase reactions, among which bubble column reactor types have attracted a huge deal of interest within the environmental, biopharmaceuticals, petrochemical, wastewater treatment, etc.^{1–5}. These versatile chemical/biochemical reactors could bring advantages as a result of decent heat and mass transfers, easy operation, and so on^{6,7}. There are numerous studies focusing on the gas–water systems for assessing hydrodynamic performance of these reactors^{8,9} and it is of vital importance to create a simulation and assess the fluid flow parameters inside the bubble columns for better process understanding. Model-based process development approach can be utilized in this context for process intensification and improvements. The findings could considerably help the engineers and researchers in design, optimization, operation, etc.^{1,10}.

Computational fluid dynamics (CFD)¹¹ is a precise approach to study two-phase fluid flow in the bubble columns, and analyze the interactions between phases, i.e. gas and liquid. CFD simulations have been utilized in various studies^{12–14} to assess these types of reactors containing water and air systems. Due to the presence of two phases inside the reactor and interaction between them, almost all studies considered the Eulerian CFD model and just the mass transfer in the reactor both internally and between phases^{7,15–17}. According to literature, there are no CFD studies considering non-equilibrium thermal conditions between air and water in a bubble column reactor. This case study is considered, for the first time, in the present paper. The temperature difference between air and water adds the energy governing equations to the CFD modeling to build the comprehensive simulation methodology. Considering the interphase heat transfer between gas and liquid makes CFD modeling of the reactor more complicated, and sophisticated methods are required.

Besides, according to the literature, artificial intelligence (AI) methods are helpful ways for enhancement of applications of the CFD modeling^{18–22}. A few studies have already reported the usage of ANFIS model with the CFD for the prediction of fluid flow characteristics in various circumstances^{23–28}. Although the PSOFIS method has been already investigated for the data optimizations in many engineering aspects^{29–32}, there are no investigations adopted the PSOFIS in cooperation with the CFD modeling. For example, Shi and Eberhart²⁹ reported the potential of the PSOFIS by benchmarking the experimental data. Hu et al.³⁰ performed the PSOFIS to minimize the power loss in electricity distribution systems. We investigated the effects of parameters of the PSOFIS on the best intelligence in detail. Therefore, the AI method of particle swarm optimization (PSO) algorithm based fuzzy inference system (PSOFIS) is selected in this work to help the CFD modeling. In order to achieve the most accurate prediction of the algorithm, the values of input numbers, swarm sizes, and inertia weights are investigated. The increase of the mesh density is also tested for the first time by the PSOFIS. An additional comparison is made between PSOFIS and ANFIS results regarding the accuracy of the methods.

Methodology

Geometry of the reactor. A cylindrical column is considered with a diameter of 29 cm and a length of 2 m here for the computational tasks and understanding the process. In this reactor, the existing gas phase (air) is sent to the column of water from the bottom. Air velocity and air temperature are respectively 0.02 m/s and 400 K, while the water temperature is 295 K.

CFD approach. The Eulerian–Eulerian two-phase model was utilized in this work with the two-equation standard $k - \varepsilon$ turbulence model. In this fluid modeling approach, the following equations are derived for each phase inside the reactor¹²:

- Continuity equation of phase k :

$$\frac{\partial}{\partial t}(\epsilon_k \rho_k) + \frac{\partial}{\partial x_i}(\epsilon_k \rho_k u_{k,i}) = 0. \quad (1)$$

- Momentum equation of phase k :

$$\frac{\partial}{\partial t}(\epsilon_k \rho_k u_{k,i}) + u_j \frac{\partial}{\partial x_j}(\epsilon_k \rho_k u_{k,i}) = -\epsilon_k \frac{\partial P}{\partial x_i} + \epsilon_k \rho_k g + \frac{\partial}{\partial x_j} \left(\epsilon_k (\mu + \mu_t) \frac{\partial u_{k,i}}{\partial x_j} \right) + F_I \quad (2)$$

The energy equation is used to calculate the interphase heat transfer between air and water³³.
Energy equation of phase k :

$$\frac{\partial \rho_k \epsilon_k H_k}{\partial t} + \nabla \cdot (\rho_k \epsilon_k u_{k,i} H_k) = \nabla [\epsilon_k (k + k_t)(\nabla T_k)] + Q_I. \quad (3)$$

The momentum interphase interactions are the summation of the drag force and the turbulent dispersion defining as follows:

$$\begin{aligned} F_I &= F_{td} + F_d \\ F_{td} &= -C_{td} \rho_{water} k \nabla \epsilon_{water}, \end{aligned} \quad (4)$$

where k and C_{td} are the water turbulent kinetic energy per unit of mass and turbulent dispersion coefficient, respectively. The value of 0.3 is considered for the turbulent dispersion coefficient based on the study of²².

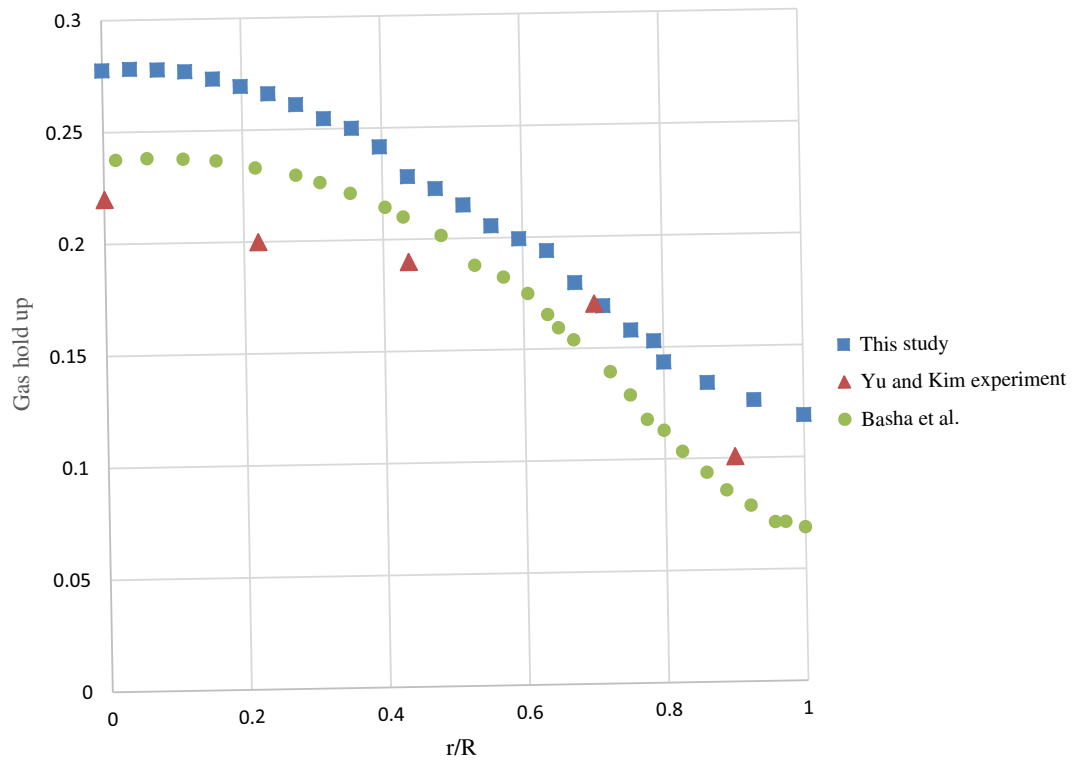


Figure 1. Validation of present CFD study versus Yu and Kim experiment and numerical investigation of Basha et al.

$$F_d = \frac{1}{8} C_D a_{if} \rho_k |\vec{u}_{k,i} - \vec{u}_{i,k}| (\vec{u}_{k,i} - \vec{u}_{i,k}), \tag{5}$$

$$Q_I = h a_{if} (T_{k,i} - T_{i,k}). \tag{6}$$

The Schiller-Naumann^{34,35} drag coefficient (C_D) is adopted for inter-phase interaction of the momentum equations, while for interphase heat transfer coefficient (h) between air bubble and water, the Ranz-Marshall³⁶ equation is used. It should be noted that the air is considered as incompressible fluid and the bubble shape is supposed to be spherical. So, the interphase area (a_{if}) is given as follows:

$$a_{if} = \frac{6 \epsilon_{air}}{d_{air\ bubble}}. \tag{7}$$

In this study, the standard $k - \epsilon$ turbulence model was selected. The key mathematical models utilized in the present work taken from the literature³⁷⁻⁴²:

$$\frac{\partial}{\partial t} (\epsilon_k \rho_k k_k) + \nabla \cdot (\epsilon_k \rho_k u_{k,i} k_k) = \nabla \cdot \left[\left(\frac{\mu_k^t}{\sigma_k} \right) \nabla (k_k) \right] + G_k - \rho_k \epsilon_k, \tag{8}$$

$$\frac{\partial}{\partial t} (\epsilon_k \rho_k \epsilon_k) + \nabla \cdot (\rho_k \epsilon_k u_{k,i}) = \nabla \cdot \left[\frac{\mu_k^t}{\sigma_\epsilon} \nabla \epsilon_k \right] + \frac{\epsilon_k}{k_k} (C_{1\epsilon} G_k - C_{2\epsilon} \rho_k \epsilon_k), \tag{9}$$

$$G_k = \mu_k^t (\nabla u_{k,i} + (\nabla u_{k,i})^T), \tag{10}$$

$$\mu_k^t = \rho_k C_\mu \frac{k^2}{\epsilon}. \tag{11}$$

Grid partition test and validation. F the grid independency test process, two mesh arrangements are employed for the simulation of the reactor: the former with 9477 nodes and the latter with 18,954 nodes. The CFD results have been compared in the case of the water and air velocities and the deviation was less than 0.04%. For less computational efforts, the first mesh density has been adopted in this study. For verification of the CFD

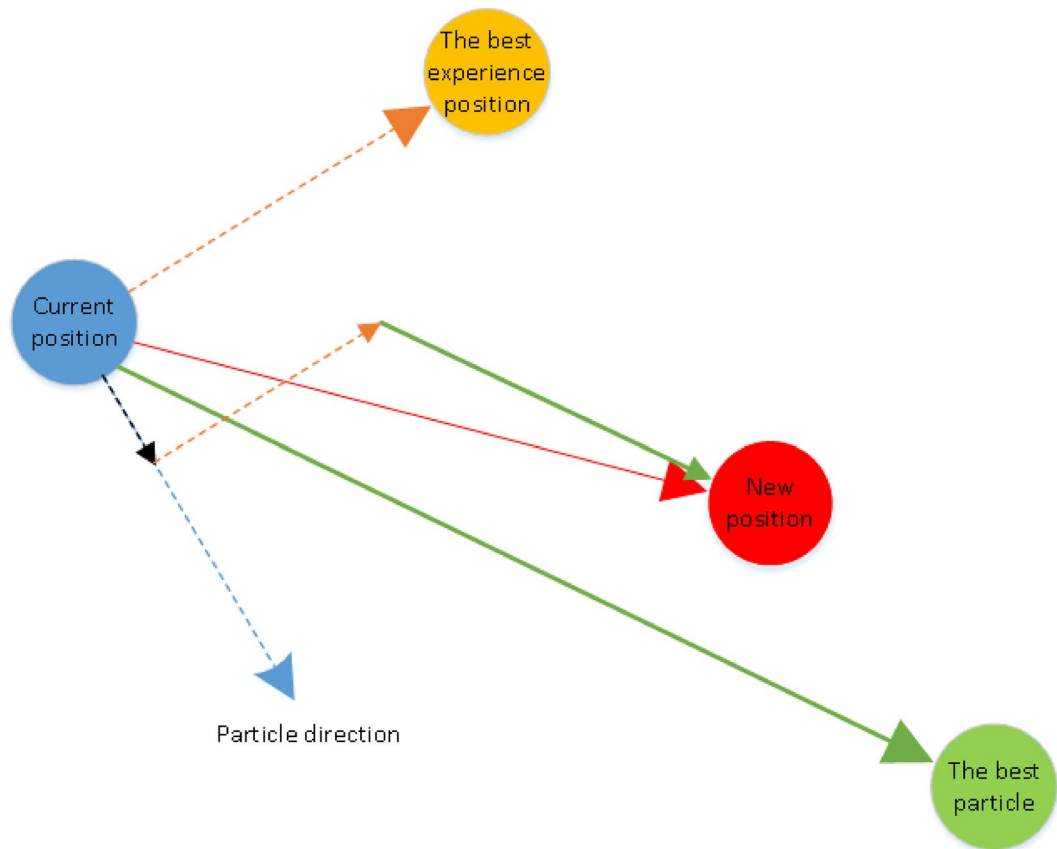


Figure 2. Schematics of PSO algorithm.

simulation, the results of gas hold-up predictions are compared with the experiment of Yu and Kim⁴³ and the numerical results of Basha et al.³⁴ (Fig. 1).

Particle swarm optimization. Particle swarm optimization (PSO) is population-based algorithms that generate and use random variables. This algorithm has been inspired by the collective behavior of animals like the group of birds or fishes. In this method the population of animals and the candidate solutions are known as swarm and particles, respectively⁴⁴. The PSO algorithm is based on the collective behavior of individuals in a community (Fig. 2). This means that there are a number of individuals, namely particles here, searching for the best place as a target or output variable for prediction in the community. Every particle has its own velocity, and it is done its own search iteratively for finding the best place. The best place is known as the solution or the prediction of the output variable. During the searching process of each individual particle, finding the new place is affected by two factors; the former is the best experience of the particle until that iteration; the latter is the best experience among all particles together.

The optimal location found for a particle is recorded and called *pbest*. The best position finding by the whole particles is called *gbest*. Taking *pbest*, *gbest* and each particle's velocity, the update rule for their location is as follows^{45–47}:

$$V_{t+1} = W_t \times V_t + C_1 \times \text{rand}() \times (pbest - x_t) + C_2 \times \text{rand}() \times (gbest - x_t), \quad (12)$$

$$x_{t+1} = x_t + V_{t+1}, \quad (13)$$

where W represents the inertia weight showing the impact of the fr velocity vector (V_t) on the new vector, C_1 and C_2 denote the acceleration constants and $\text{rand}()$ represents a random function in the range $[0, 1]$ and x_t denotes the present location of the pticle.

Table 1 summarizes the parameters of the PSO algorithms that are used in this study. The values of swarm size and inertia weight are adjusted in order the best intelligence to be achieved, while the inertia weight damping ratio, the personal and the global learning coefficients have been fixed in the model.

Fuzzy inference system (FIS). FIS is a fuzzy engine in terms of the concepts of fuzzy if–then rules, and fuzzy set theory. In this intelligence approach, if–then rules presented by Takagi and Sugeno are run⁴⁸. In this

PSO algorithm parameters	
Swarm size	60, 80, 100, 120
Inertia weight (0–1)	0.85, 0.9, 0.95, 1
Inertia weight damping ratio	0.99
Personal learning coefficient (0–2)	1
Global learning coefficient (0–2)	2

Table 1. Particle swarm optimization algorithm parameters.

Fuzzy inference system parameters	
Percentage of data for training (P)	76%
Number of data	9477
Iteration	400
Data clustering method	FCM clustering
Membership function (MF)	Gaussmf
Number of cluster (NC)	30
Number of rules and output MFs	30

Table 2. Fuzzy inference system parameters.

study x coordination, y coordination and z coordination are taken to attain liquid phase velocity as output. The k th rule function is:

$$w_k = \mu_{xk}(X)\mu_{yk}(Y)\mu_{zk}(Z). \quad (14)$$

The detailed procedure is reported elsewhere^{17–19,48}.

The fuzzy set parameters are described in Table 2. Totally, there are 9477 data that are created by the CFD simulation. 76% of the generated data are learned and the prediction is done after 400 iterations. The fuzzy C-means clustering is adopted as the cluster type. The type of membership function is Gaussian. The number of clusters, the rules, and the output membership function all is 30.

Results and discussion

Two-phase air–water flow inside a bubble column type chemical reactor is simulated via CFD method. The air is injected into the bubble column filling with water⁴⁹. For the first time in this study, the temperature of the air (127 °C) differs from the water (23 °C). As a result, there is not any thermal equilibrium between air and water. This requires the additional governing equation of energy for the CFD modeling. All governing equations (i.e. mass, momentum, energy, turbulence model) are considered in the Eulerian–Eulerian framework for the simulation of process. This means the equations are solved for each phase separately and coupled with each other in the source terms. Therefore, solving two-phase CFD models, the 3D modeling, considering the effect of turbulent flow imposes massive computational efforts. The PSO algorithm-based fuzzy inference system (PSOFIS) was selected for the CFD modeling simplification.

Figure 3 illustrates the flowchart of the PSO algorithm designed for this study. PSOFIS learns the CFD data generated by the numerical simulations for the prediction of a specific variable as the output (target). In the present study, liquid phase (i.e. water) velocity is the output value. The x , y , and z coordinates of the nodes' location of the water are the inputs. 76% of the whole CFD data (i.e. 9477 data) is trained by the PSOFIS, while the 100% CFD data are used in testing. The regression is adopted as an index for reaching the best intelligence. Different input numbers (i.e. 1, 2, and 3), swarm sizes (i.e. 60, 80, 100, and 120), and inertia weights (i.e. 0.85, 0.9, 0.95, and 1) are tested for achieving the best intelligence. Figure 4 shows the influence of input numbers on the regression number. As the number of input increases, the regression numbers go up for both training and testing. The best intelligence is achieved when the input number is equal to 3 (i.e. $R = 0.98$).

A similar sensitivity test is done for the effect of swarm sizes, and inertia weights when the input number is 3. Figure 5 illustrates the PSOFIS learning processes with considering changes in swarm size when number of inputs is 3. According to this figure, by increasing swarm sizes from 60 to 100, the R value increases from 0.97 to 0.98. However, the further increases of swarm size to 120, no significant changes are seen in the value of R .

Figure 6 depicts the PSOFIS learning processes with considering changes in inertia weight when swarm size is 100 and number of inputs is 3. Regarding this figure, rising inertia weights from 0.85 to 1, the R value

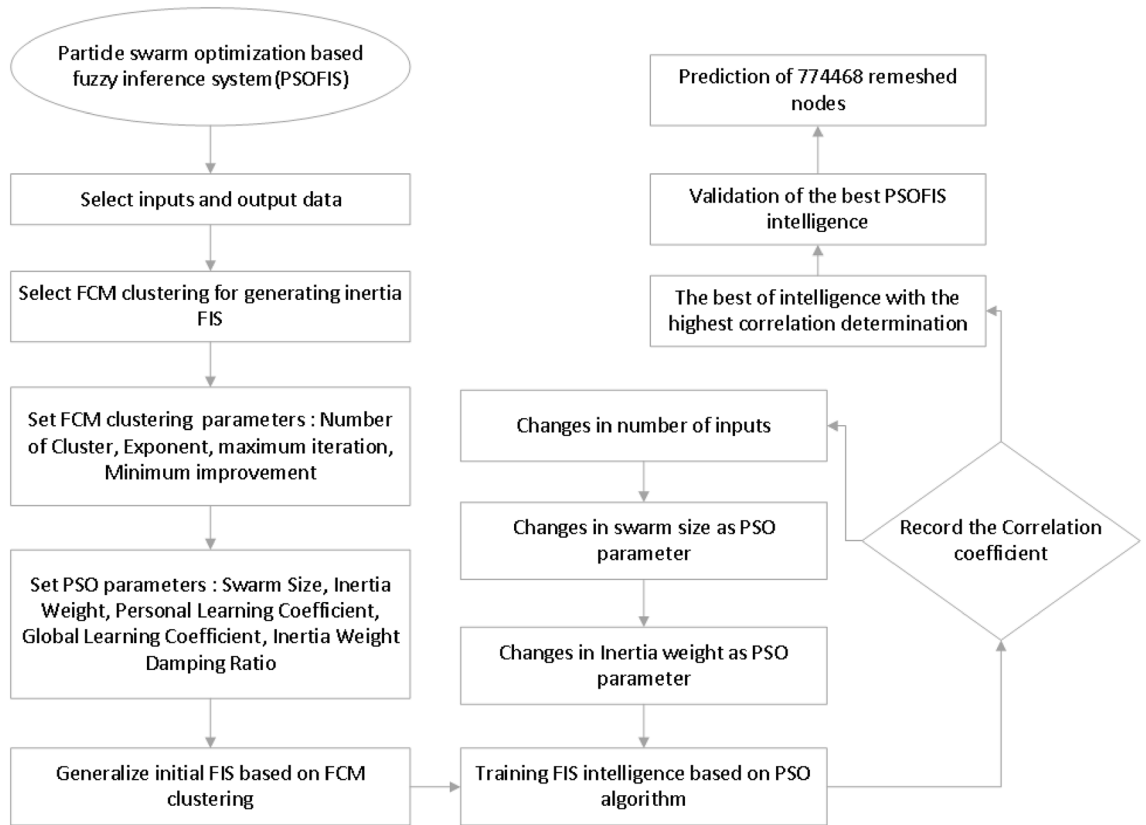


Figure 3. Schematics of combination of PSO algorithm and fuzzy inference system.

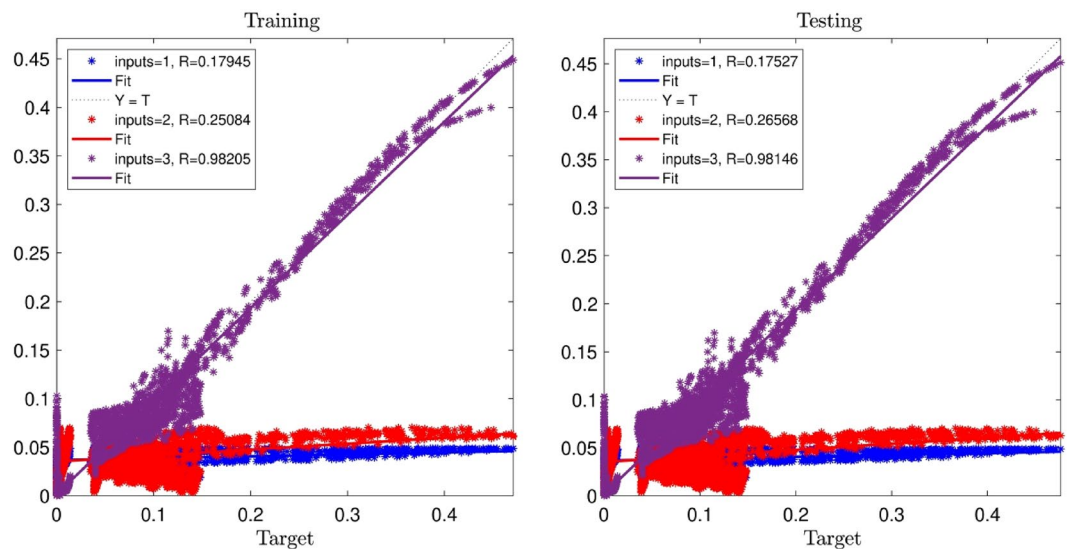


Figure 4. PSOFIS learning processes with considering changes in number of inputs.

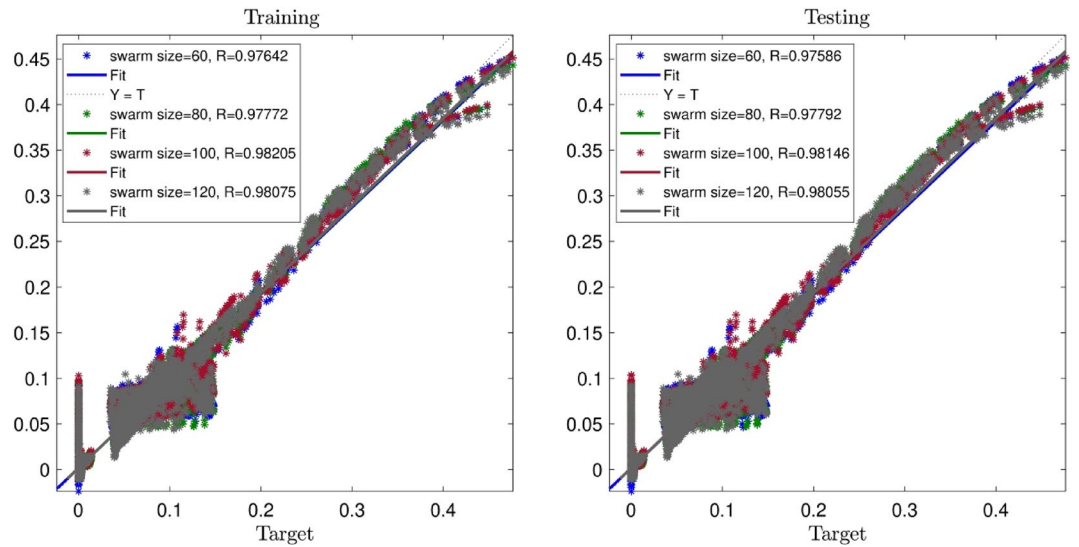


Figure 5. PSOFIS learning processes with considering changes in swarm size when number of inputs is 3.

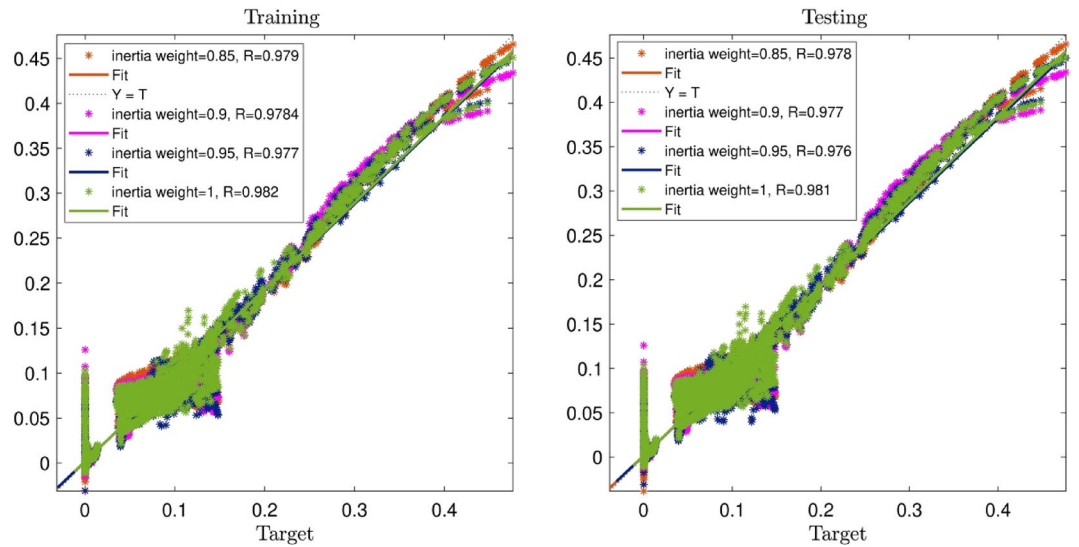


Figure 6. PSOFIS learning processes with considering changes in inertia weight when swarm size is 100 and number of inputs is 3.

increases from 0.97 to 0.98. Hence, the best intelligence can be obtained for the input number of 3, swarm size of 100, and inertia weight of 1.

For more validation, the integration of the adaptive network with the fuzzy inference system, calling ANFIS, is employed for learning the CFD outcomes for simulating of the water velocity inside the reactor⁴⁹. The results of the PSOFIS are compared with the ANFIS. It should be noted that for the similar setup condition, all the

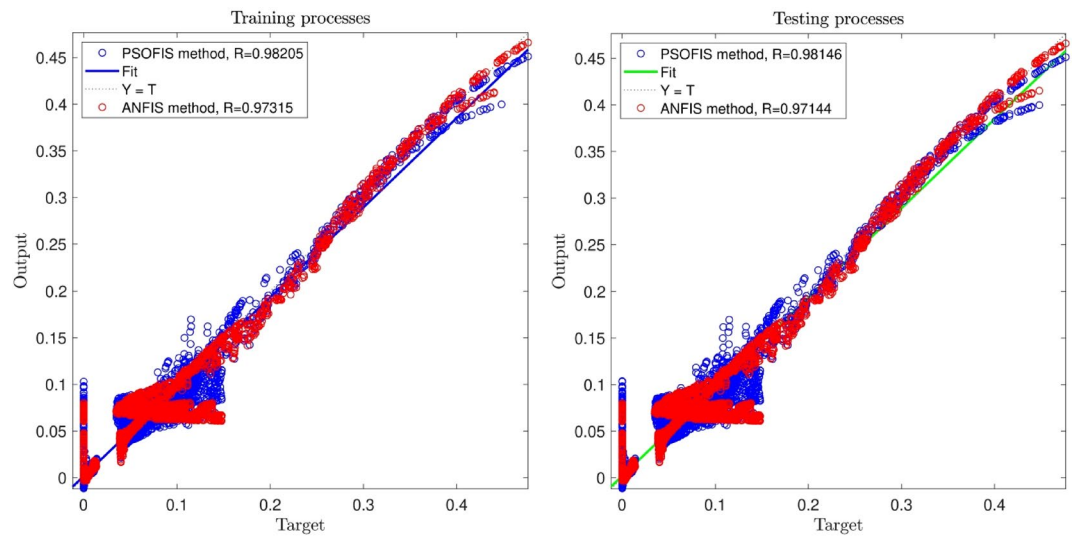


Figure 7. Comparison of the best result of PSOFIS and ANFIS methods.

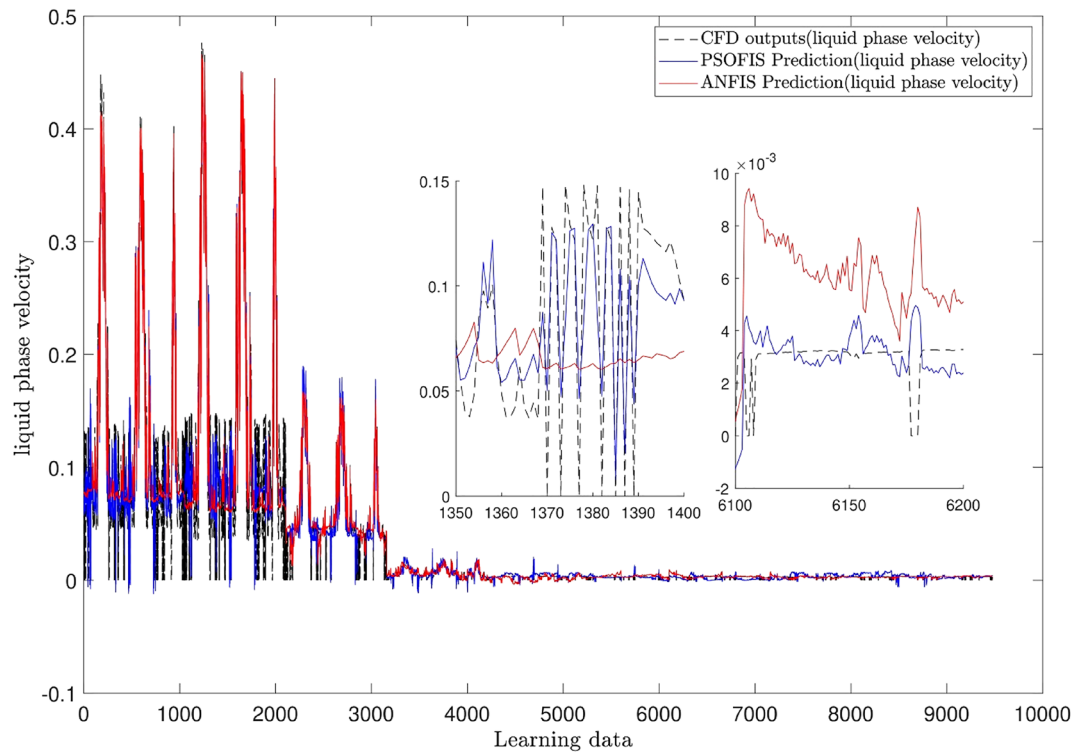


Figure 8. Pattern of liquid phase velocity in different methods.

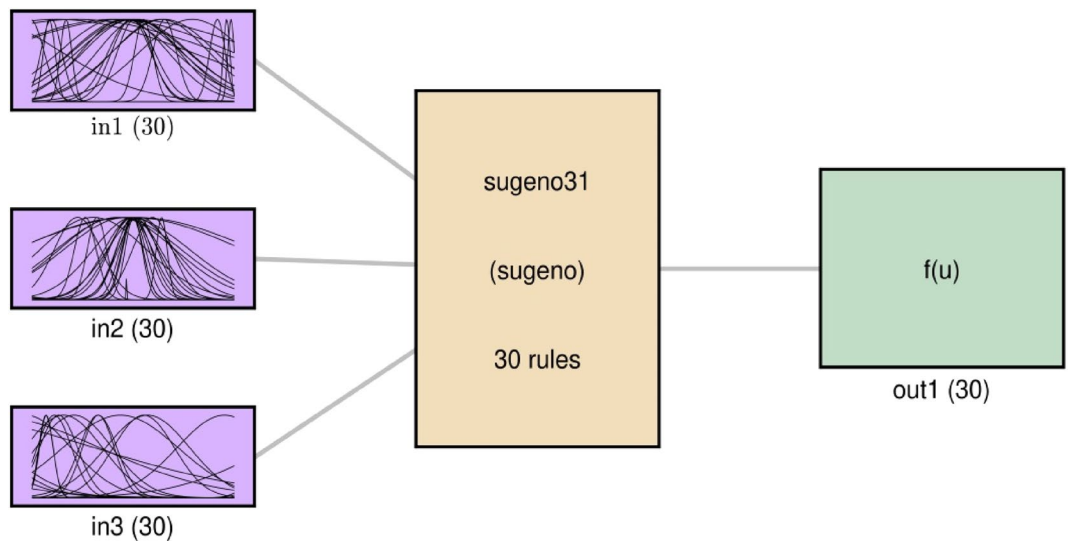


Figure 9. FIS structure using PSO algorithm as trainer in learning process.

fuzzy set parameters of the ANFIS are the same as the PSOFIS (referring to Table 2). According to Fig. 7, the R value of the PSOFIS (0.98) is a little more than that of the ANFIS (0.97). Figure 8 illustrates the pattern of the liquid phase velocity in both methods of ANFIS and PSOFIS. Magnifying the graphs, it is seen that the PSOFIS predictions follow the CFD results with more compatibility in comparison with the ANFIS.

The FIS structure based on PSO learning process is shown in Fig. 9 in a schematic way. The membership function is Gaussian as shown in input boxes on the right. The number of clusters in for each input, the number of rules in the hidden layer, and the number of membership functions for output are 30. The type of cluster is fuzzy semi clustering.

Figures 10a–c illustrate the comparison between the CFD and the PSOFIS predictions of water velocity in each input. As seen, there is no conflict between the results of both methods. Since the results are for the time of 30 s, as to be expected, the water velocity is higher at lower heights of the column (i.e. $z = 0.1$ and 0.2 m) and the velocity is damped to reach zero at higher heights (i.e. $z = 0.9$ m).

After reaching the best intelligence, the water velocity can be found for more nodes in the column domain without mesh refinement in the CFD domain. In fact, the mesh refinement can be done in the PSOFIS with much less computational efforts. Figure 11 illustrates the increase of the mesh density from 9477 to 774,468 nodes using the PSOFIS method.

The results of the PSOFIS predictions of the water velocity are depicted in Fig. 12. The new predictions of the PSOFIS method are in agreement again with the CFD results. Moreover, additional predictions of the water velocity in more nodes are seen in Fig. 12a–c.

Conclusions

The two-phase flow of air–water inside a bubble column reactor with a non-equilibrium thermal condition between air and water was simulated by the CFD method. The hot air with a temperature of 127 °C was injected into the water column with a temperature of 23 °C. The Eulerian two-phase CFD model was implemented for turbulent flow inside the bubble column. The artificial intelligence algorithm and in specific the particle swarm optimization (PSO) algorithm-based fuzzy inference system (PSOFIS) was employed to help such complicated CFD modeling. A lot of computational cost, effort, and time are saved by the reduction of the number of CFD simulations. Once the best intelligence is achieved, no need for simulation anymore.

The PSOFIS was used to predict the water velocity at x , y , and z nodes positions in the column. The regression number was considered as an index for the best intelligence. The proper values of input numbers, swarm

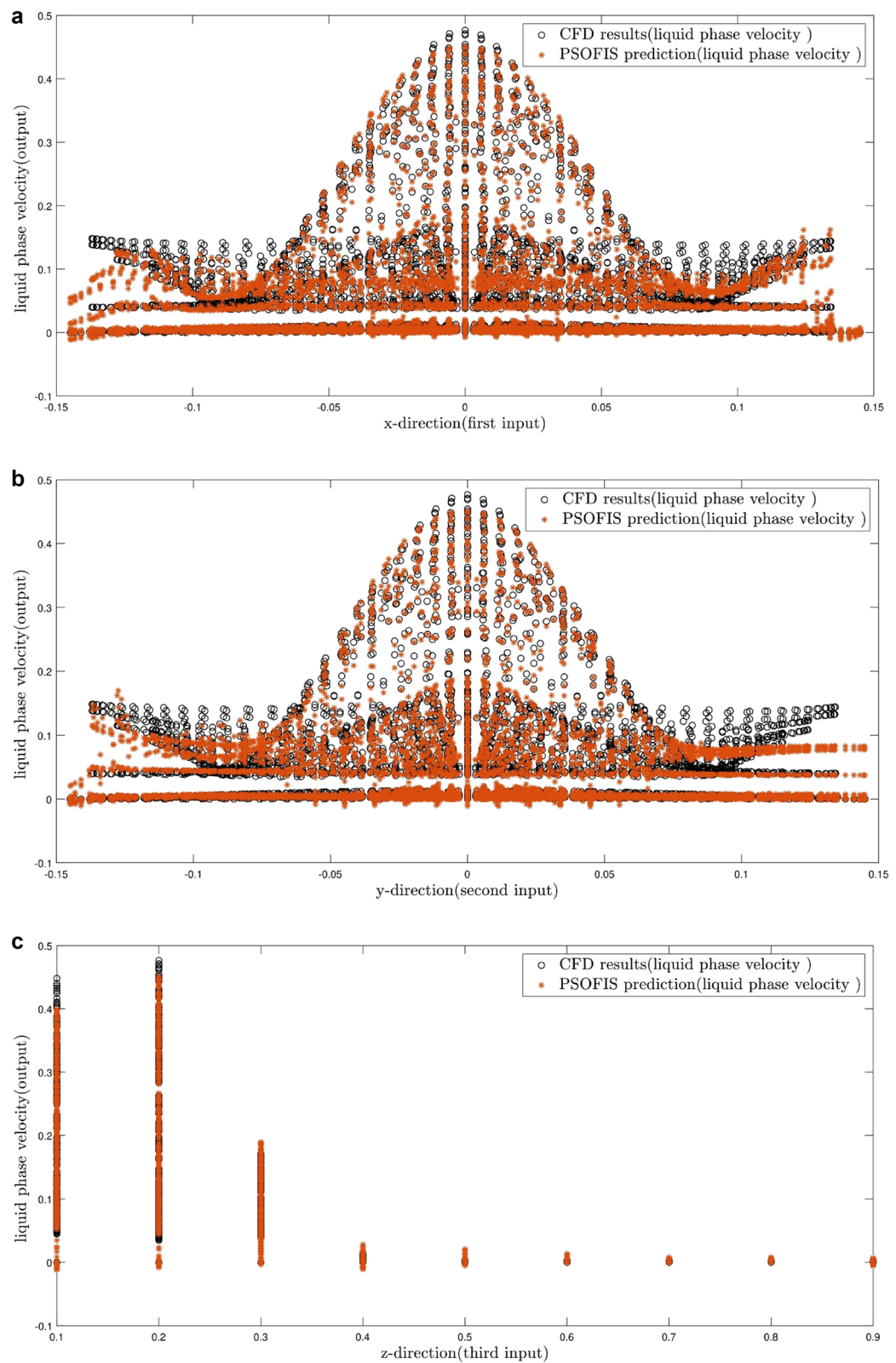


Figure 10. (a) Validation of PSOFIS learning process after achieving the highest PSOFIS intelligence based on first input. (b) Validation of PSOFIS learning process after achieving the highest PSOFIS intelligence based on second input. (c) Validation of PSOFIS learning process after achieving the highest PSOFIS intelligence based on third input.

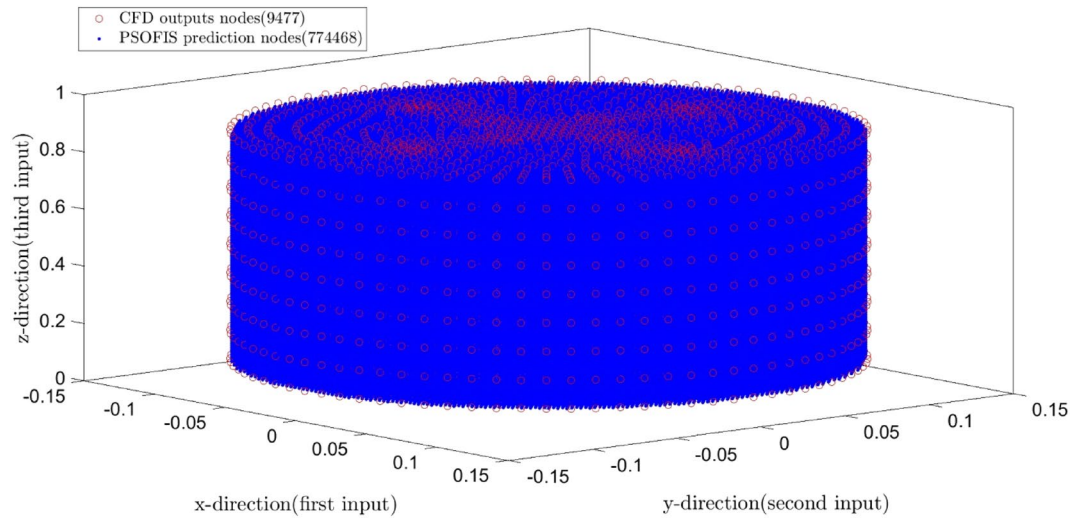


Figure 11. Remeshed domain from 9477 to 774,468.

sizes, and inertia weights were investigated for the best intelligence. For more validation, the integration of the adaptive network with the fuzzy inference system (ANFIS) was used for learning the CFD data. The results of the PSOFIS were compared with the ANFIS for the same fuzzy set parameters.

At the best intelligence of the PSOFIS, the water velocity was found for additional nodes without mesh refinement in the CFD domain. In fact, the mesh refinement could be done in the PSOFIS with much less computational efforts.

The results of this study are summarized as follows:

- The best intelligence is found for the input number of 3, swarm size of 100, and inertia weight of 1 where the regression number is around 0.98.
- The PSOFIS predictions follow the CFD results with more compatibility in comparison with the ANFIS. The regression number (R) of the PSOFIS (0.98) was more than that of the ANFIS (0.97).

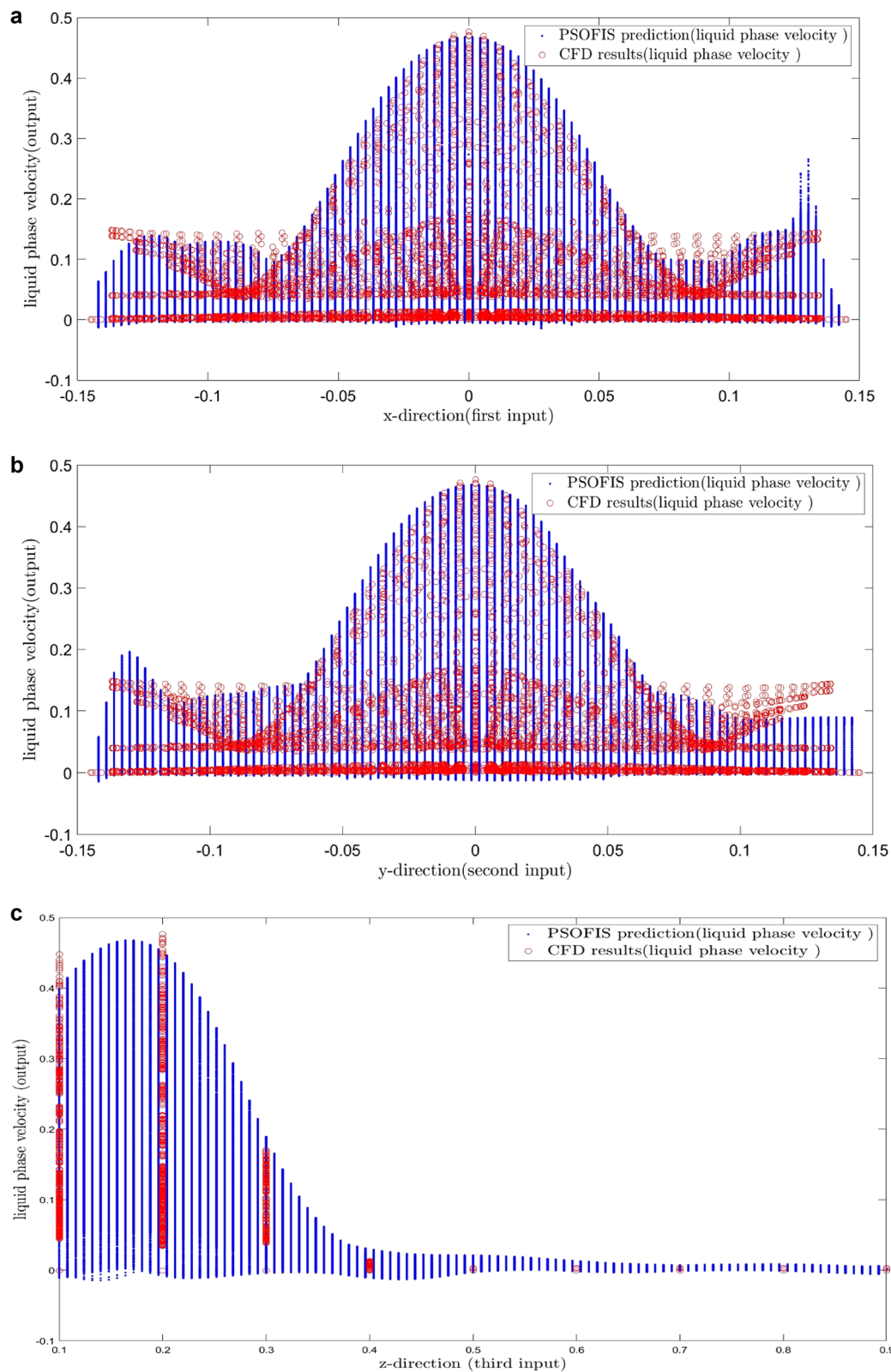


Figure 12. (a) Liquid phase velocity prediction of PSOFS in 774,468 nodes based on first input. (b) Liquid phase velocity prediction of PSOFS in 774,468 nodes based on second input. (c) Liquid phase velocity prediction of PSOFS in 774,468 nodes based on third input.

- Comparison between the CFD and the PSOFIS predictions of water velocity shows no conflict between the results of both methods.
- The prediction of the water velocity shows a logic trend by increasing the height of the column. As expected, the water velocity is higher at lower heights of column (i.e. $z = 0.1$ and 0.2 m) and the velocity is damped to reach zero at higher heights (i.e. $z = 0.9$ m).
- Increasing mesh density of the bubble column from 9477 to 774,468 by the PSOFIS method, the new prediction of the PSOFIS method covers all the CFD results with additional predictions of the water velocity in more nodes in the domain.

Received: 26 August 2020; Accepted: 4 January 2021

Published online: 15 January 2021

References

1. Rollbusch, P. *et al.* Bubble columns operated under industrially relevant conditions—current understanding of design parameters. *Chem. Eng. Sci.* **126**, 660–678 (2015).
2. Duduković, M. P., Larachi, F. & Mills, P. L. Multiphase catalytic reactors: A perspective on current knowledge and future trends. *Catal. Rev.* **44**, 123–246 (2002).
3. Ge, W. & Li, J. Macro-scale phenomena reproduced in microscopic systems—Pseudo-particle modeling of fluidization. *Chem. Eng. Sci.* **58**, 1565–1585 (2003).
4. Wu, Y. & Gidaspow, D. Hydrodynamic simulation of methanol synthesis in gas–liquid slurry bubble column reactors. *Chem. Eng. Sci.* **55**, 573–587 (2000).
5. Smith, J. S. & Valsaraj, K. T. Bubble column reactors for wastewater treatment. 3. Pilot-scale solvent sublation of pyrene and pentachlorophenol from simulated wastewater. *Ind. Eng. Chem. Res.* **36**, 903–914 (1997).
6. Anastasiou, A., Passos, A. & Mouza, A. Bubble columns with fine pore sparger and non-Newtonian liquid phase: Prediction of gas holdup. *Chem. Eng. Sci.* **98**, 331–338 (2013).
7. Wang, T. & Wang, J. Numerical simulations of gas–liquid mass transfer in bubble columns with a CFD–PBM coupled model. *Chem. Eng. Sci.* **62**, 7107–7118 (2007).
8. Monahan, S. M. Computational fluid dynamics analysis of air–water bubble columns (2007).
9. Monahan, S. M. & Fox, R. O. Linear stability analysis of a two-fluid model for air–water bubble columns. *Chem. Eng. Sci.* **62**, 3159–3177 (2007).
10. Krishna, R. & Sie, S. Design and scale-up of the Fischer-Tropsch bubble column slurry reactor. *Fuel Process. Technol.* **64**, 73–105 (2000).
11. Al-Baali, A.A.-G. & Farid, M. M. *Sterilization of Food in Retort Pouches* 33–44 (Springer, Berlin, 2006).
12. Yan, P. *et al.* Numerical simulation of bubble characteristics in bubble columns with different liquid viscosities and surface tensions using a CFD–PBM coupled model. *Chem. Eng. Res. Des.* **154**, 47–59 (2020).
13. Bhusare, V., Dhiman, M., Kalaga, D. V., Roy, S. & Joshi, J. B. CFD simulations of a bubble column with and without internals by using OpenFOAM. *Chem. Eng. J.* **317**, 157–174 (2017).
14. Pourtousi, M., Sahu, J. & Ganesan, P. Effect of interfacial forces and turbulence models on predicting flow pattern inside the bubble column. *Chem. Eng. Process.* **75**, 38–47 (2014).
15. Wehinger, G. D., Peeters, J., Muzafarjia, S., Eppinger, T. & Kraume, M. Numerical simulation of vertical liquid-film wave dynamics. *Chem. Eng. Sci.* **104**, 934–944 (2013).
16. Liu, Y. & Hinrichsen, O. Study on CFD–PBM turbulence closures based on k – ϵ and Reynolds stress models for heterogeneous bubble column flows. *Comput. Fluids* **105**, 91–100 (2014).
17. Babanezhad, M., Nakhjiri, A. T., Rezakazemi, M. & Shirazian, S. Developing intelligent algorithm as a machine learning overview over the big data generated by Euler-Euler method to simulate bubble column reactor hydrodynamics. *ACS Omega* **5**, 20558 (2020).
18. Babanezhad, M., Pishnamazi, M., Marjani, A. & Shirazian, S. Bubbly flow prediction with randomized neural cells artificial learning and fuzzy systems based on k – ϵ turbulence and Eulerian model data set. *Sci. Rep.* **10**, 1–12 (2020).
19. Babanezhad, M., Nakhjiri, A. T. & Shirazian, S. Changes in the number of membership functions for predicting the gas volume fraction in two-phase flow using grid partition clustering of the ANFIS method. *ACS Omega* **5**, 16284–16291 (2020).
20. Zeinali, M., Mazlan, S. A., Choi, S.-B., Imaduddin, F. & Hamdan, L. H. Influence of piston and magnetic coils on the field-dependent damping performance of a mixed-mode magnetorheological damper. *Smart Mater. Struct.* **25**, 055010 (2016).
21. Pourtousi, M., Zeinali, M., Ganesan, P. & Sahu, J. N. Prediction of multiphase flow pattern inside a 3D bubble column reactor using a combination of CFD and ANFIS. *RSC Adv.* **5**, 85652–85672. <https://doi.org/10.1039/c5ra11583c> (2015).
22. Pourtousi, M., Sahu, J. N., Ganesan, P., Shamshirband, S. & Redzwan, G. A combination of computational fluid dynamics (CFD) and adaptive neuro-fuzzy system (ANFIS) for prediction of the bubble column hydrodynamics. *Powder Technol.* **274**, 466–481. <https://doi.org/10.1016/j.powtec.2015.01.038> (2015).
23. Nguyen, Q., Babanezhad, M., Taghvaie Nakhjiri, A., Rezakazemi, M. & Shirazian, S. Prediction of thermal distribution and fluid flow in the domain with multi-solid structures using Cubic-interpolated pseudo-particle model. *PLoS ONE* **15**, e0233850 (2020).
24. Babanezhad, M., Taghvaie Nakhjiri, A., Rezakazemi, M. & Shirazian, S. Developing intelligent algorithm as a machine learning overview over the big data generated by Euler-Euler method to simulate bubble column reactor hydrodynamics. *ACS Omega* **5**, 20558 (2020).
25. Varol, Y., Koca, A., Oztop, H. F. & Avci, E. Analysis of adaptive-network-based fuzzy inference system (ANFIS) to estimate buoyancy-induced flow field in partially heated triangular enclosures. *Expert Syst. Appl.* **35**, 1989–1997 (2008).
26. Varol, Y., Avci, E., Koca, A. & Oztop, H. F. Prediction of flow fields and temperature distributions due to natural convection in a triangular enclosure using adaptive-network-based fuzzy Inference System (ANFIS) and Artificial Neural Network (ANN). *Int. Commun. Heat Mass Transfer* **34**, 887–896 (2007).
27. Nguyen, Q., Behroyan, I., Rezakazemi, M. & Shirazian, S. Fluid Velocity Prediction inside bubble column reactor using ANFIS algorithm based on CFD input data. *Arab. J. Sci. Eng.* **45**, 7487 (2020).
28. Nguyen, Q., Taghvaie Nakhjiri, A., Rezakazemi, M. & Shirazian, S. Thermal and flow visualization of a square heat source in a nanofluid material with a cubic-interpolated pseudo-particle. *ACS Omega* **5**, 17658 (2020).
29. Shi, Y. & Eberhart, R. C. In *Proc. 2001 Congress on Evolutionary Computation (IEEE Cat. No. 01TH8546)* 101–106 (IEEE).
30. Hu, W., Chen, Z., Bak-Jensen, B. & Hu, Y. Fuzzy adaptive particle swarm optimisation for power loss minimisation in distribution systems using optimal load response. *IET Gener. Transm. Distrib.* **8**, 1–10 (2014).
31. Neshat, M. FAIPSO: Fuzzy adaptive informed particle swarm optimization. *Neural Comput. Appl.* **23**, 95–116 (2013).
32. Niknam, T., Mojjarrad, H. D. & Nayeripour, M. A new fuzzy adaptive particle swarm optimization for non-smooth economic dispatch. *Energy* **35**, 1764–1778 (2010).

33. Laborde-Boutet, C. *et al.* CFD simulations of hydrodynamic/thermal coupling phenomena in a bubble column with internals. *Aiche J.* **56**, 2397–2411 (2010).
34. Basha, O. M., Weng, L., Men, Z. & Morsi, B. I. CFD modeling with experimental validation of the internal hydrodynamics in a pilot-scale slurry bubble column reactor. *Int. J. Chem. Reactor Eng.* **14**, 599–619 (2016).
35. Law, D., Battaglia, F. & Heindel, T. J. Model validation for low and high superficial gas velocity bubble column flows. *Chem. Eng. Sci.* **63**, 4605–4616 (2008).
36. Liao, Y., Krepper, E. & Lucas, D. A baseline closure concept for simulating bubbly flow with phase change: A mechanistic model for interphase heat transfer coefficient. *Nucl. Eng. Des.* **348**, 1–13 (2019).
37. Bhole, M., Joshi, J. & Ramkrishna, D. CFD simulation of bubble columns incorporating population balance modeling. *Chem. Eng. Sci.* **63**, 2267–2282 (2008).
38. Díaz, M. E. *et al.* Numerical simulation of the gas–liquid flow in a laboratory scale bubble column: Influence of bubble size distribution and non-drag forces. *Chem. Eng. J.* **139**, 363–379 (2008).
39. Ekambara, K. & Dhotre, M. CFD simulation of bubble column. *Nucl. Eng. Des.* **240**, 963–969 (2010).
40. Nakhjiri, A. T. & Roudsari, M. H. Modeling and simulation of natural convection heat transfer process in porous and non-porous media. *Appl. Res. J.* **2**, 199–204 (2016).
41. Fan, W., Yuan, L. & Li, Y. CFD Simulation of flow pattern in a bubble column reactor for forming aerobic granules and its development. *Environ. Technol.* **40**, 3652–3667 (2019).
42. Behroyan, I., Ganesan, P., He, S. & Sivasankaran, S. CFD models comparative study on nanofluids subcooled flow boiling in a vertical pipe. *Numer. Heat Transfer A Appl.* **73**, 55–74 (2018).
43. Yu, Y. H. & Kim, S. D. Bubble characteristics in the radial direction of three-phase fluidized beds. *J. Am. Inst. Chem. Eng.* <https://doi.org/10.1002/aic.690341217> (1988).
44. Nedjah, N. & de Macedo Mourelle, L. *Swarm Intelligent Systems* Vol. 26 (Springer, Berlin, 2006).
45. Shi, Y. & Eberhart, R. C. *Annual Conference on Evolutionary Programming* 591–600 (Springer, Berlin, Heidelberg, 1994).
46. Shi, Y. & Eberhart, R. In *1998 IEEE International Conference on Evolutionary Computation Proceedings. IEEE World Congress on Computational Intelligence (Cat. No.98TH8360)* 69–73.
47. Nguyen, N. T., Kim, C.-G. & Janiak, A. *Intelligent Information and Database Systems* (Springer, Berlin, 2011).
48. Takagi, T. & Sugeno, M. Fuzzy identification of systems and its applications to modeling and control. *IEEE Trans. Syst. Man Cybern.* **1**, 116–132 (1985).
49. Babanezhad, M. *et al.* High-performance hybrid modeling chemical reactors using differential evolution based fuzzy inference system. *Sci. Rep.* **10**(1), 21304 (2020).

Acknowledgements

Saeed Shirazian gratefully acknowledges the supports by the Government of the Russian Federation (Act 211, contract 02.A03.21.0011) and the Ministry of Science and Higher Education of the Russian Federation (Grant FENU-2020-0019).

Author contributions

M.B.: Conceptualization, Simulations, Writing-draft. I.B.: Modeling, Analysis, Validation. A.T.N.: Methodology, Software. A.M.: Supervision. M.R.: Writing-review, Revision. A.H.b: Analysis, Validation. S.S.: Supervision, Funding acquisition, Modeling.

Competing interests

The authors declare no competing interests.

Additional information

Correspondence and requests for materials should be addressed to A.M.

Reprints and permissions information is available at www.nature.com/reprints.

Publisher's note Springer Nature remains neutral with regard to jurisdictional claims in published maps and institutional affiliations.



Open Access This article is licensed under a Creative Commons Attribution 4.0 International License, which permits use, sharing, adaptation, distribution and reproduction in any medium or format, as long as you give appropriate credit to the original author(s) and the source, provide a link to the Creative Commons licence, and indicate if changes were made. The images or other third party material in this article are included in the article's Creative Commons licence, unless indicated otherwise in a credit line to the material. If material is not included in the article's Creative Commons licence and your intended use is not permitted by statutory regulation or exceeds the permitted use, you will need to obtain permission directly from the copyright holder. To view a copy of this licence, visit <http://creativecommons.org/licenses/by/4.0/>.

© The Author(s) 2021